Research Square

Preprints are preliminary reports that have not undergone peer review.
They should not be considered conclusive, used to inform clinical practice,
or referenced by the media as validated information.

Recombinant Expression of Cliotide U1 in Pichia pastoris: Antibacterial Activity and Mechanistic Insights

Xiao-Ya Wang
Tianjin University of Science and Technology
Yun-Zhi Li
Tianjin University of Science and Technology
Hao-Yang Dong
Tianjin University of Science and Technology
Zi-Xin Wang
Tianjin University of Science and Technology
Xin-lei Chu
Tianjin Medical University Cancer Institute and Hospital, Tianjin Medical University
Chun-Ming Dong
mingchundongjy@tust.edu.cn

Tianjin University of Science and Technology

Research Article

Keywords: Cliotide U1, Pichia pastoris, recombinant expression, antibacterial activity, membrane disruption

Posted Date: November 26th, 2026

DOI: https://doi.org/10.21203/rs.3.rs-11508057/v1

License: This work is licensed under a Creative Commons Attribution 4.0 International License.
Read Full License

Additional Declarations: No competing interests reported.

Recombinant Expression of Cliotide U1 in Pichia pastoris: Antibacterial Activity and Mechanistic Insights

Xiao-Ya Wang[a], Yun-Zhi Li[a], Hao-Yang Dong[a], Zi-Xin Wang[a], Xin-lei Chu[b*], Chun-Ming Dong[a*]

[a] College of Marine and Environmental Sciences, Tianjin University of Science and Technology, Tianjin 300457, China

[b] Department of Epidemiology and Biostatistics, Tianjin Medical University Cancer Institute and Hospital, Tianjin Medical University, Tianjin 300060, China

***Corresponding authors:**

Chun-Ming Dong (mingchundongjy@tust.edu.cn); Xin-lei Chu (chuxinlei2014@163.com).

***Correspondence addresses:**

College of Marine and Environmental Sciences, Tianjin University of Science and Technology, Tianjin 300457, China; Department of Epidemiology and Biostatistics, Tianjin Medical University Cancer Institute and Hospital, Tianjin Medical University, Tianjin 300060, China.

Author contributions:

Xiao-Ya Wang: Investigation, Methodology, Formal analysis, Writing – original draft.

Yun-Zhi Li: Data curation, Writing – original draft.

Hao-Yang Dong: Software, Formal analysis.

Zi-Xin Wang: Conceptualization, Supervision, Writing – review and editing.

Xin-lei Chu: Conceptualization, Supervision, Writing – review and editing.

Chun-Ming Dong: Conceptualization, Supervision, Writing – review and editing.

Abstract

Antimicrobial resistance has increased the need for new antibacterial agents and scalable production methods. Cliotide U1 (CU1), a plant-derived antimicrobial peptide, has reported activity against Gram-positive and Gram-negative bacteria, but its production has relied on low-yield extraction or chemical synthesis. Here, CU1 was recombinantly expressed in Pichia pastoris, and the antibacterial activity and properties of the CU1-containing fermentation supernatant (CU1-FS) were characterized. CU1-FS inhibited all six tested bacterial strains, with apparent minimum inhibitory concentrations of 3 – 8 μg/mL based on ELISA-estimated His-tagged products. Antibacterial activity was retained to varying degrees after temperature, pH, salt, and protease treatments, and CU1-FS showed low hemolysis of human erythrocytes under the tested conditions. Scanning electron microscopy showed changes in bacterial cell morphology; propidium iodide staining and measurements of extracellular nucleic acid- and protein-associated absorbance supported increased membrane permeability and leakage of intracellular components. Agarose gel electrophoresis showed altered migration of bacterial genomic DNA, consistent with a potential in vitro interaction. Molecular docking and 100-ns molecular dynamics simulations provided predicted interaction models for CU1 with selected bacterial proteins and a model lipid membrane. Because the tested material was unpurified CU1-FS, contributions from other supernatant components cannot be excluded. These findings establish a recombinant production approach for bioactive CU1-containing supernatant and support further study of CU1-associated membrane effects.

Keywords: Cliotide U1; *Pichia pastoris*; recombinant expression; antibacterial activity; membrane disruption

1 Introduction

In recent years, the One Health approach has become an increasingly important framework for global public health, emphasizing coordinated prevention and risk management based on the interconnected health of humans, animals, and the environment. Against this background, antimicrobial resistance (AMR) has emerged as a major global public health challenge spanning clinical, agricultural, and environmental settings [1,2]. Antibiotics are essential for the prevention and treatment of bacterial infections and are widely used in human medicine, livestock production, and aquaculture. However, their prolonged and inappropriate use exerts sustained selective pressure on microbial populations, promoting the emergence and spread of resistance and reducing the effectiveness of existing antibacterial treatments [3]. Global antibiotic consumption has increased substantially over recent decades [4], and demand may continue to rise with population growth, expanding healthcare needs, and agricultural development. Without effective interventions, drug-resistant infections will impose an increasing disease burden and further limit treatment options for common bacterial infections [5]. In intensive aquaculture systems, water and sediments can serve as reservoirs and transmission pathways for antibiotic resistance genes, while continuous antibiotic exposure may further promote the emergence and dissemination of environmental resistance [6,7]. Similarly, excessive antibiotic use in livestock production contributes to the selection and spread of resistant bacteria, which, together with resistance genes, may reach humans through environmental contamination, direct animal contact, and the food chain [8]. Antimicrobial peptides (AMPs) have attracted increasing attention as potential alternatives to conventional antibiotics because of their structural diversity, rapid antibacterial activity, and ability to act through multiple mechanisms, offering new opportunities to address the challenges posed by AMR [9,10].

Antimicrobial peptides (AMPs) are a diverse group of low-molecular-weight bioactive peptides widely found in plants, animals, and microorganisms, and constitute an important component of innate defense systems [11,12]. Unlike many conventional antibiotics that act on specific molecular targets, AMPs often exhibit rapid bactericidal activity and act through multiple mechanisms, which may reduce the likelihood of resistance development [13]. Some AMPs initially interact with negatively charged bacterial surfaces through electrostatic attraction and subsequently disturb the lipid bilayer, increasing membrane permeability and causing the leakage of intracellular contents. Others can enter bacterial cells and interact with intracellular targets, including DNA, RNA, ribosomes, proteins, and metabolic enzymes, thereby interfering with nucleic acid synthesis, protein translation, and other essential cellular processes. The ability of AMPs to act on both bacterial membranes and intracellular components makes them attractive candidates for the development of new antibacterial agents [14]. Despite these advantages, the development of AMPs remains limited by production efficiency and manufacturing costs. Chemical synthesis can produce peptides with defined sequences, but the costs and purification difficulties increase with peptide length, structural complexity, and production scale [15]. Among the available expression systems, *Escherichia coli* is widely used for recombinant protein production because of its rapid growth, low cultivation costs, and well-established genetic tools. However, the expression of certain AMPs in *E. coli* can be limited by toxicity to the host, proteolytic degradation, improper folding, and poor protein solubility [16,17]. In contrast, yeast expression systems combine the advantages of microbial cultivation with the capacity for eukaryotic protein folding, processing, and secretion, providing an alternative platform for producing bioactive peptides and recombinant proteins [18]. Among these systems, *Pichia pastoris* (currently classified as *Komagataella phaffii*) has become an important

host for heterologous protein and peptide production owing to its ability to grow at high cell densities, well-established genetic manipulation techniques, and efficient secretory expression capabilities [19].

Cliotide U1 (CU1) is a plant-derived antimicrobial peptide isolated and characterized from the leaves of *Urtica dioica* by Taheri et al. in 2025 [20]. The native peptide exhibits antibacterial activity against both Gram-positive and Gram-negative bacteria, with minimum inhibitory concentrations (MICs) ranging from 1 to 4 μM, along with thermal stability, low cytotoxicity, and low hemolytic activity. Despite these properties, several limitations remain. Extraction from its natural source is inefficient, yielding only approximately 5 mg of purified CU1 from 400 g of *U. dioica* leaves, corresponding to approximately 0.06% of the total leaf protein [20]. Furthermore, an established heterologous expression system capable of reliably producing biologically active CU1 is still lacking. Its antibacterial mechanism also remains incompletely understood, particularly regarding membrane disruption, intracellular effects, and potential molecular interactions [20].

To address these limitations, this study aimed to establish a recombinant expression system for CU1 in *Pichia pastoris* and obtain recombinant products with antibacterial activity. The antibacterial spectrum, minimum inhibitory concentrations (MICs), physicochemical stability, and hemolytic activity were systematically evaluated. The antibacterial mechanism was further investigated at the cellular and molecular levels through bacterial phenotypic assays, DNA interaction analysis, molecular docking, and molecular dynamics simulations.

2 Materials and Methods

2.1 Strains and Plasmids

Pichia pastoris GS115 was used as the host for heterologous expression of CU1, while *Escherichia coli* XL10-Gold was used for cloning and propagation of recombinant plasmids. The recombinant expression construct was generated using the laboratory-maintained pPICZαA plasmid as the vector backbone.

The bacterial strains used in antibacterial activity assays and related functional experiments included *Listeria monocytogenes* ATCC 21633, *Salmonella* sp. ATCC 10467, *E. coli* ATCC 10305, *E. coli* O157 ATCC 35150, *Staphylococcus aureus* ATCC 25923, and *Bacillus subtilis* ATCC 6633. All strains were maintained in our laboratory.

2.2 Bioinformatics Analysis

The amino acid sequence of Cliotide U1 (CU1), LIVAASLVYDFYTWIAKKVALLRIAKKVLYLARNA, was obtained from the native peptide reported by Taheri et al. [20]. The physicochemical properties of CU1, including molecular weight, theoretical isoelectric point (pI), numbers of charged amino acid residues, instability index, aliphatic index, and grand average of hydropathicity (GRAVY), were calculated using ExPASy ProtParam [21]. The secondary structure was predicted using SOPMA [22], and the three-dimensional structure was modeled using PEP-FOLD3 [23]. The hydrophobicity profile of CU1 was analyzed using ExPASy ProtScale based on the Kyte–Doolittle hydropathy scale [24]. Potential phosphorylation sites at serine (Ser), threonine (Thr), and tyrosine (Tyr) residues were predicted using NetPhos 3.1 [25]. SignalP 6.0 was used to assess the N-terminal signal peptide features [26], while DeepTMHMM was employed to predict transmembrane topology [27]. Potential toxicity and allergenicity were predicted using ToxinPred and AllerTOP v2.1, respectively [28,29].

2.3 Construction and Verification of Recombinant Pichia pastoris Strains

The coding sequence of CU1 was optimized according to its amino acid sequence and the codon usage preferences of P. pastoris [30]. The codon-optimized CU1 gene was synthesized by GENEWIZ (Suzhou, China) and cloned into the pPICZαA vector to generate the recombinant expression plasmid pPICZαA–CU1. The resulting plasmid was transformed into E. coli XL10-Gold for propagation. Positive colonies were selected and inoculated into LB medium containing 25 μg/mL Zeocin, followed by incubation at 37 °C and 220 rpm for approximately 12 h. After cultivation, the recombinant plasmid was extracted using a plasmid extraction kit according to the manufacturer's instructions and stored at −20 °C until further use.

The recombinant plasmid pPICZαA–CU1 was linearized with SacI at 37 °C for 12 h. The digestion products were analyzed by electrophoresis on a 1% agarose gel, and the linearized DNA was recovered by gel purification. P. pastoris GS115 was activated in YPD medium and cultured at 30 °C and 220 rpm until the optical density at 600 nm (OD600) reached 0.8–1.1. The cells were harvested by centrifugation, treated with a prechilled LiAc-DTT/sorbitol solution, washed with 1 mol/L sorbitol, and resuspended in prechilled 1 mol/L sorbitol to prepare competent cells. The linearized pPICZαA–CU1 plasmid was introduced into GS115 competent cells by chemical transformation. Following incubation at 30 °C, DMSO was added, and the transformation mixture was incubated at 42 °C for 15 min. YPD liquid medium was then added, and the cells were allowed to recover at 30 °C and 220 rpm for 1 h. The recovered cells were spread onto YPD agar plates containing 25 μg/mL Zeocin and incubated at 30°C for 48–72 h. Individual colonies were subsequently transferred to YPD agar plates containing 100 μg/mL Zeocin for further selection.

Genomic DNA was extracted from candidate transformants for PCR verification. The forward primer pPICZa-6his-up (5′-GGTTCTCATCATCATCATCATCATGATGATGATGATAAG-3′) and

reverse primer pPIC-Cliotide U1-dn (5′-TTAAGCGTTTCTAGCCAAGTA-3′) were used for amplification. Each PCR reaction was performed in a total volume of 20 μL containing 10 μL of 2× PCR Mix, 2 μL of genomic DNA, 2 μL of each primer, and 4 μL of sterile water. The amplification program consisted of an initial denaturation at 95 °C for 5 min, followed by 30 cycles of denaturation at 94 °C for 1 min, annealing at 54 °C for 1 min, and extension at 72 °C for 1 min, with a final extension at 72 °C for 10 min. PCR products were analyzed by electrophoresis on a 1% agarose gel. A P. pastoris transformant carrying the empty pPICZαA vector was used as the negative control. PCR-positive transformants were further verified by DNA sequencing, and the obtained sequences were compared with the designed CU1 coding sequence. Recombinant strains with confirmed sequences were preserved in glycerol stocks at −80 °C.

2.4 Induced Expression of Recombinant CU1

A single colony of the sequence-verified recombinant Pichia pastoris GS115 strain was inoculated into 5 mL of BMGY medium and cultured at 30 °C and 220 rpm for 24 h. The culture was then transferred into 100 mL of fresh BMGY medium at a 1:20 inoculation ratio and incubated for another 12–16 h until the OD600 reached 0.8–1.0. Cells were harvested by centrifugation, washed with sterile water, and resuspended in 100 mL of BMMY medium for methanol induction at 30 °C and 220 rpm. Methanol was supplemented every 24 h to maintain a final concentration of 1%, and induction was continued for 6 days. Samples were collected at 24 h intervals throughout the induction period (D1–D6). Following centrifugation to remove the cells, the culture supernatants were filtered through a 0.22 μm membrane and used for subsequent expression analysis and antibacterial activity assays. Staphylococcus aureus ATCC 25923 was used as the indicator strain to compare the antibacterial activity of culture supernatants collected at different induction times.

2.5 Identification and Quantification of Recombinant CU1

The expression of recombinant CU1-related products in the culture supernatant was examined, and their concentrations were estimated for subsequent antibacterial and functional assays. Culture supernatant samples were subjected to Tricine‐SDS‐PAGE analysis. Before electrophoresis, samples were heated at 100℃ for 15 min. Electrophoresis was initially performed at 80 V, and the voltage was increased to 140 V after the samples entered the resolving gel [31]. Following electrophoresis, proteins were transferred onto a polyvinylidene difluoride (PVDF) membrane using a wet transfer system. After blocking, the membrane was sequentially incubated with an anti-His-tag mouse monoclonal antibody (1:2000) and an HRP-conjugated goat anti-mouse IgG secondary antibody (1:5000). Immunoreactive bands were detected using an enhanced chemiluminescence (ECL) substrate to confirm the presence of His-tagged recombinant products in the culture supernatant.

The concentration of His-tagged recombinant products in the culture supernatant was further estimated using an enzyme-linked immunosorbent assay (ELISA) based on His-tag recognition. A standard curve was generated using His-tagged green fluorescent protein (GFP) at known concentrations. The standards and recombinant CU1-containing culture supernatants were separately added to 96-well microplates, followed by coating, blocking, and antibody incubation. After the addition of 3,3′,5,5′-tetramethylbenzidine (TMB) substrate, absorbance was measured at 450 nm. The apparent concentration of His-tagged recombinant products in the culture supernatant was estimated from the standard curve [32]. The estimated concentrations were used to determine the sample concentrations for subsequent antibacterial activity, hemolytic activity, and mechanistic assays using CU1-containing fermentation supernatant (CU1-FS).

2.6 Antibacterial Activity and MIC Determination

The antibacterial activity of CU1-containing fermentation supernatant (CU1-FS) was evaluated using the agar well diffusion assay. The tested bacterial strains included Listeria monocytogenes ATCC 21633, Salmonella sp. ATCC 10467, Escherichia coli ATCC 10305, E. coli O157 ATCC 35150, Staphylococcus aureus ATCC 25923, and Bacillus subtilis ATCC 6633. Activated bacterial cultures were uniformly spread onto agar plates, and 100 μL of CU1-FS was added to each well. CU1-free control fermentation supernatant was used as the negative control. Antibacterial activity was assessed by observing the formation of inhibition zones after incubation.

The minimum inhibitory concentration (MIC) was determined using the broth microdilution method. Bacterial suspensions were adjusted to approximately 1×10^6 CFU/mL and mixed with different concentrations of CU1-FS in 96-well microplates. Following incubation at 37 °C for approximately 16 h, the MIC was defined as the lowest CU1-FS concentration at which no visible bacterial growth, as indicated by the absence of turbidity, was observed.

2.7 Stability Assessment

The antibacterial activity of CU1-FS following exposure to different treatment conditions was evaluated using the agar well diffusion assay, with Staphylococcus aureus as the indicator strain. For thermal stability assessment, CU1-FS was incubated at 4, 25, 37, 50, 60, 80, and 100 °C for 1 h. After cooling to room temperature, the antibacterial activity was determined. CU1-FS incubated at 4 °C for 1 h served as the reference, while CU1-free control fermentation supernatant was used as the negative control.

To evaluate the effect of pH, CU1-FS was adjusted to pH 2, 6, 8, 10, or 12 and incubated at 37 °C for 1 h before testing its antibacterial activity. A pH 8 buffer control and CU1-free control

fermentation supernatant adjusted to pH 8 were included as controls.

Salt tolerance was assessed by supplementing CU1-FS with NaCl at concentrations of 0, 50, 150, 300, and 500 mmol/L, where 0 mmol/L indicated no additional NaCl. All samples were incubated at 37 °C for 1 h before antibacterial activity was measured.

For protease stability assessment, CU1-FS was separately mixed with equal volumes of pepsin, proteinase K, papain, or trypsin solutions and incubated at 37 °C for 1 h. The enzymes were subsequently inactivated by heating in a dry block heater, and the samples were cooled to room temperature before antibacterial activity was determined. Untreated CU1-FS, buffer, and CU1-free control fermentation supernatant were included as controls.

All treatments were evaluated under the same antibacterial assay conditions, and antibacterial activity was compared by measuring the diameters of the inhibition zones.

2.8 Hemolytic Activity Assay

The hemolytic activity of CU1-FS was evaluated using a human erythrocyte hemolysis assay. Fresh blood samples were obtained from healthy donors at Tianjin University of Science and Technology. Erythrocytes were collected by centrifugation, washed with phosphate-buffered saline (PBS), and resuspended to obtain a 4% (v/v) erythrocyte suspension. CU1-FS samples were prepared at concentrations of 0.78, 1.58, 3.15, 6.3, and 12.6 μg/mL. For each treatment, 100 μL of the prepared sample was mixed with 900 μL of the erythrocyte suspension and incubated at 37 °C for 1 h. After incubation, the mixtures were centrifuged, and the absorbance of the collected supernatants was measured at 540 nm. PBS and 1% Triton X-100 were used as the negative and positive controls, respectively. The percentage of hemolysis was calculated using the following equation:

$$\text{Hemolysis (\%)} = \frac{A_{\text{sample}} - A_{\text{negative}}}{A_{\text{positive}} - A_{\text{negative}}} \times 100\%$$

where A_sample, A_negative, and A_positive represent the absorbance values at 540 nm of the CU1-FS-treated samples, the PBS negative control, and the 1% Triton X-100 positive control, respectively.

2.9 Analysis of the Antibacterial Mechanism of CU1

2.9.1 Scanning Electron Microscopy

Scanning electron microscopy (SEM) was used to examine changes in bacterial cell surface morphology following CU1-FS treatment. Staphylococcus aureus and Escherichia coli were selected as representative bacterial strains. Exponentially growing bacterial cultures were treated with CU1-FS at 1× MIC for 1 h, while cultures treated with CU1-free control fermentation supernatant served as controls. After treatment, bacterial cells were harvested, washed with buffer, and fixed with glutaraldehyde. The samples were then dehydrated sequentially using an ethanol series of 30%, 50%, 70%, and 100%. Following drying and sample preparation, bacterial surface morphology was examined by SEM, and morphological differences between the treated and control groups were compared.

2.9.2 Assessment of Membrane Permeability by PI Staining

Propidium iodide (PI) fluorescence staining was performed to evaluate the effect of CU1-FS on bacterial membrane permeability. Exponentially growing cultures of S. aureus and E. coli were treated with CU1-FS at 1× MIC for 1 h. PI was subsequently added to a final concentration of 50 μg/mL, and the samples were incubated in the dark for 1 h. Following staining, fluorescence images were acquired using a fluorescence microscope. Bacterial cultures treated with CU1-free control fermentation supernatant were used as controls. Changes in PI fluorescence signals between the

treated and control groups were compared to assess bacterial membrane permeability.

2.9.3 Leakage of Intracellular Components

The effect of CU1-FS on bacterial membrane integrity was further evaluated by measuring the leakage of intracellular components, following a previously reported method with modifications [33]. A single colony of S. aureus was inoculated into LB broth and cultured at 37 °C and 220 rpm until the exponential growth phase. The bacterial culture was centrifuged at 4000 rpm for 5 min at room temperature. The harvested cells were washed with phosphate-buffered saline (PBS), and the bacterial suspension was adjusted to 1.0×10^8 CFU/mL.

For the concentration-dependent assay, equal volumes of the bacterial suspension and CU1-FS at concentrations of 0.39, 0.79, 1.58, 3.15, 6.3, and 12.6 μg/mL were mixed and incubated at 37 °C for 3 h. After treatment, bacterial cells were removed by centrifugation, and the supernatants were collected. Absorbance at 260 and 280 nm was measured using a microvolume spectrophotometer to assess the release of nucleic acid-related and protein-related intracellular components, respectively.

For the time-dependent assay, the bacterial suspension was mixed with undiluted CU1-FS and incubated at 37 °C. Samples were collected after 1, 2, 3, and 4 h of incubation. At each time point, bacterial cells were removed by centrifugation, and the absorbance of the collected supernatants was measured at 260 and 280 nm. Bacterial suspensions treated with CU1-free control fermentation supernatant and 0.1% Triton X-100 served as the negative and positive controls, respectively.

2.9.4 Analysis of the Interaction Between CU1-FS and Bacterial Genomic DNA

The potential interaction between CU1-FS and bacterial genomic DNA was examined by agarose gel electrophoresis, following a previously reported method with modifications [34]. Single colonies of *Escherichia coli* and *Staphylococcus aureus* were separately inoculated into LB broth

and cultured at 37 °C and 220 rpm for 6–8 h until the exponential growth phase. Genomic DNA was extracted using a bacterial genomic DNA extraction kit according to the manufacturer's instructions, and DNA concentrations were measured using a microvolume spectrophotometer.

CU1-FS was diluted to different concentrations with phosphate-buffered saline (PBS). Each reaction contained 200 ng of bacterial genomic DNA and 20 μL of DNA-binding buffer (10 mmol/L Tris-HCl, 50 mmol/L NaCl, and 1 mmol/L EDTA; pH 8.0). CU1-FS was then added to achieve final concentrations of 3.15, 6.3, and 12.6 μg/mL. Genomic DNA incubated with CU1-free control fermentation supernatant served as the negative control. The reaction mixtures were incubated at 35 °C for 1 h, after which DNA loading buffer was added. The samples were analyzed by electrophoresis on a 1% agarose gel to examine changes in DNA migration and electrophoretic retardation, thereby assessing the potential interaction between CU1-FS and bacterial genomic DNA.

2.9.5 Molecular Docking and Molecular Dynamics Simulations

Molecular docking and molecular dynamics (MD) simulations were performed to investigate the potential interactions of CU1 with bacterial target proteins and lipid membranes. For molecular docking, the outer membrane porin F (OmpF) from *E. coli* (PDB ID: 2OMF) and sortase A from *S. aureus* (PDB ID: 1T2P) were selected as receptor proteins. Their three-dimensional structures were obtained from the RCSB Protein Data Bank, while the three-dimensional structure of CU1 was generated using the AlphaFold Server [35]. CU1 was used as the ligand and docked separately against OmpF and sortase A using the HDOCK Server [36]. Candidate binding poses were ranked according to the docking scores and confidence scores provided by HDOCK. The top-ranked pose (Model 1) from each docking system was selected for further analysis. Three-dimensional and two-dimensional visualizations were used to examine the predicted binding sites, key interacting amino

acid residues, hydrogen bonds, and other noncovalent interactions. The HDOCK docking scores were used only for relative comparisons among candidate binding poses and were not interpreted as experimentally determined binding free energies.

Molecular dynamics simulations were performed using GROMACS 2020.6-MODIFIED [37]. A lipid bilayer consisting of 150 molecules of 1-palmitoyl-2-oleoyl-sn-glycero-3-phosphoethanolamine (POPE) and 50 molecules of 1-palmitoyl-2-oleoyl-sn-glycero-3-phospho-(1′-rac-glycerol) (POPG) was constructed. CU1 was placed in the membrane environment to establish the CU1–membrane simulation system. Following energy minimization, the system was equilibrated under constant particle number, volume, and temperature (NVT) conditions, followed by constant particle number, pressure, and temperature (NPT) conditions. A 100 ns production simulation was subsequently performed. The resulting trajectories were analyzed by calculating the root mean square deviation (RMSD), radius of gyration (Rg), solvent-accessible surface area (SASA), and number of hydrogen bonds to characterize the conformational stability, structural compactness, solvent accessibility, and dynamic interactions of CU1 within the lipid bilayer environment.

3. Results and Discussion

3.1 Bioinformatic Analysis of the Sequence and Physicochemical Properties of CU1

CU1 consists of 35 amino acid residues with the sequence LIVAASLVYDFYTWIAKKVALLRIAKKVLYLARNA, corresponding to the native peptide reported by Taheri et al. [20]. Bioinformatic analysis revealed a theoretical molecular weight of 3995.90 Da and an isoelectric point (pI) of 10.12. CU1 contains six positively charged residues and

one negatively charged residue, resulting in a net charge of +5. Its grand average of hydropathicity (GRAVY) was 0.874, indicating a pronounced cationic character and relatively high overall hydrophobicity (Table 1). Toxicity and allergenicity predictions classified CU1 as "Non-Toxin" and "Probable Non-Allergen", respectively, suggesting a low predicted potential for toxicity and allergenicity.

Table 1. Physicochemical properties and predicted secondary structure of Cliotide U1 (CU1).

Parameter	Value
Amino acid length	35 aa
Molecular weight	3995.90 Da
Theoretical pI	10.12
Coding sequence length (bp)	105
Positively charged residues	6
Negatively charged residues	1
Net charge	+5
Instability index	16.52
Aliphatic index	153.43
GRAVY	0.874
α-Helix (%)	91.43%
Random coil (%)	8.57%

Note: aa, amino acids; pI, isoelectric point; GRAVY, grand average of hydropathicity. Physicochemical properties and secondary structure were predicted using ExPASy ProtParam and SOPMA, respectively.

Helical wheel analysis revealed a partial spatial segregation of hydrophobic and positively charged residues in CU1, forming relatively distinct hydrophobic and cationic faces consistent with an amphipathic structure. Kyte–Doolittle analysis further showed positive hydropathy values across most of the CU1 sequence, although the degree of hydrophobicity varied among different regions (Fig. 1A). Secondary structure prediction indicated that 32 of the 35 amino acid residues (91.43%) formed an α-helix, while the remaining three residues (8.57%) adopted a random coil conformation. The predicted three-dimensional structure was predominantly characterized by a continuous α-helical conformation (Fig. 1B).

Cationicity, hydrophobicity, and amphipathic α-helical structures are important physicochemical features associated with the membrane interactions of many antimicrobial peptides. Positively charged residues facilitate electrostatic attraction between antimicrobial peptides and negatively charged bacterial surfaces, while hydrophobic regions promote their association with the lipid bilayer [38,39]. In CU1, the net positive charge and the spatial distribution of hydrophobic residues may therefore contribute to its interaction with bacterial membranes. Its predominantly α-helical conformation could further facilitate the presentation of cationic and hydrophobic regions on different faces of the peptide, supporting interactions with both the bacterial surface and membrane lipids. These structural characteristics provide a plausible basis for the membrane-associated antibacterial activity of CU1, although sequence and structural predictions alone cannot establish its mechanism of action. Accordingly, the potential membrane-disruptive effects of CU1 were further examined through bacterial morphological observations, membrane permeability assays, and measurements of intracellular component leakage. In addition, the predicted low toxicity and allergenicity of CU1 provide preliminary safety-related information, but experimental

hemolysis assessment is necessary to evaluate its compatibility with erythrocytes.

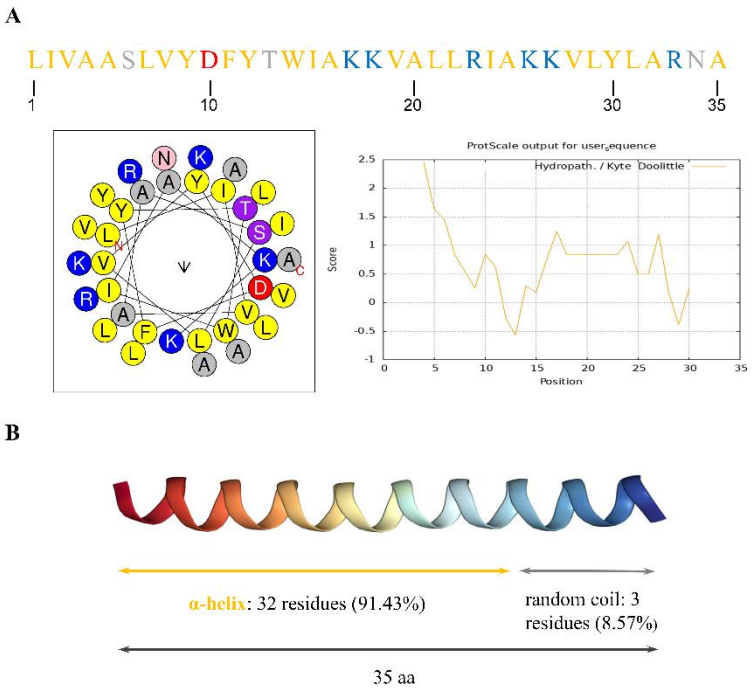


Figure 1. Sequence characteristics and predicted structural features of Cliotide U1 (CU1).

(A) Amino acid sequence, helical wheel projection, and hydropathy profile calculated using the Kyte–Doolittle scale. (B) Predicted three-dimensional structure of CU1 and its secondary structure composition, comprising 32 α-helical residues (91.43%) and three random coil residues (8.57%).

3.2 Construction and Verification of Recombinant Pichia pastoris Expressing CU1

The recombinant expression plasmid pPICZαA–CU1 was successfully constructed, with an expression cassette containing the α-factor secretion signal, Kex2 cleavage site, 6×His tag, and CU1 coding sequence (Fig. 2A). Following restriction enzyme digestion, agarose gel electrophoresis revealed a clear shift in plasmid migration compared with the undigested plasmid, consistent with successful linearization of pPICZαA–CU1 (Fig. 2B). PCR analysis of candidate *Pichia pastoris*

transformants showed amplification products of the expected size in the positive transformants, whereas no corresponding amplification product was detected in the negative control (Fig. 2C). Subsequent sequence verification confirmed the presence of the CU1 coding sequence, establishing recombinant *P. pastoris* strains carrying the target gene.

Pichia pastoris has been widely used for the recombinant production of heterologous proteins and antimicrobial peptides because of its well-established genetic manipulation tools, secretory expression capacity, and suitability for high-cell-density cultivation [40,41]. The successful construction of CU1-expressing recombinant strains provides the basis for subsequent induction and antibacterial activity assays. It also establishes a recombinant expression platform for CU1, offering a potential alternative to the low-yield extraction of the native peptide from plant material.

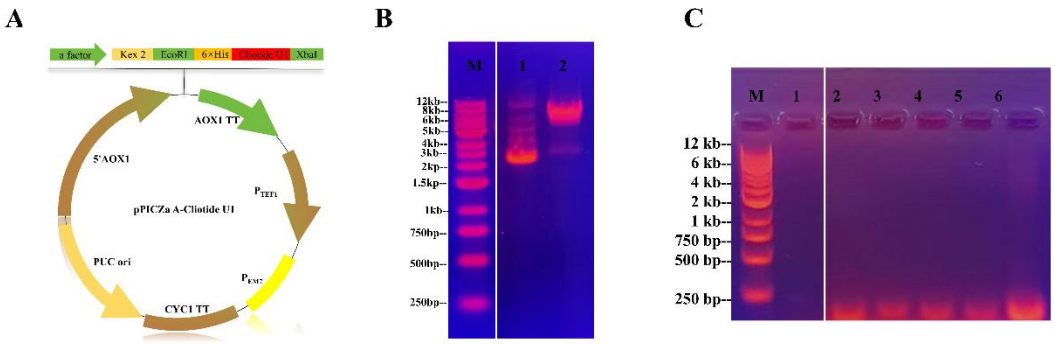


Figure 2. Construction and verification of recombinant *Pichia pastoris* strains carrying the CU1 gene. (A) Schematic representation of the recombinant pPICZαA–CU1 plasmid and its expression cassette. (B) Agarose gel electrophoresis of pPICZαA–CU1 before and after *SacI* digestion. M, DNA size marker; lane 1, undigested pPICZαA–CU1; lane 2, *SacI*-linearized pPICZαA–CU1. (C) PCR verification of candidate *P. pastoris* transformants. M, DNA size marker;

lane 1, negative control (*P. pastoris* carrying the empty pPICZαA vector); lanes 2–6, PCR products amplified from genomic DNA of five candidate transformants.

3.3 Induced Expression and Antibacterial Activity of Recombinant CU1

Following methanol induction of the recombinant *Pichia pastoris* strains, the antibacterial activity of the culture supernatants was evaluated using *Staphylococcus aureus* ATCC 25923 as the indicator strain. The culture supernatant collected on day 5 was selected for subsequent concentration estimation and functional characterization. *Pichia pastoris* has been successfully used for the secretory expression of several antimicrobial peptides, yielding recombinant products with biological activity [42]. Anti-His-tag immunoblotting of the day 5 culture supernatant revealed an immunoreactive signal, indicating the presence of His-tagged recombinant products. Subsequent ELISA analysis based on His-tag recognition yielded an apparent concentration of approximately 12.6 μg/mL, which was used to calculate the sample concentrations for subsequent experiments. Together with the observed antibacterial activity, these results confirmed that the culture supernatant obtained from the induced recombinant strain contained antibacterial components.

The antibacterial activity of the day 5 culture supernatant (CU1-FS) was further evaluated against six bacterial strains. CU1-FS produced clear inhibition zones against *Listeria monocytogenes*, *S. aureus*, *Bacillus subtilis*, *Salmonella sp*., *E. coli* O157, and *E. coli* (Fig. 3A), demonstrating antibacterial activity against both Gram-positive and Gram-negative bacteria tested in this study. MIC determination showed that the MICs of CU1-FS against *L. monocytogenes*, *S. aureus*, and *B. subtilis* were 3, 4, and 4 μg/mL, respectively, whereas those against *Salmonella* sp., *E. coli* O157, and *E. coli* were 6, 6, and 8 μg/mL, respectively (Fig. 3B). The overall MIC range

was 3 – 8 μg/mL, with *L. monocytogenes* showing the greatest susceptibility among the tested strains. Differences in susceptibility may be associated with variations in cell envelope composition, surface charge, and membrane lipid organization, which can influence the interactions between antimicrobial peptides and bacterial cells [43].

Taheri et al. reported that native CU1 exhibited antibacterial activity against a range of Gram-positive and Gram-negative bacteria, with MICs of 1 – 4 μM [20]. Similarly, CU1-FS obtained in the present study was active against both bacterial groups, with antibacterial activity further demonstrated against *L. monocytogenes, B. subtilis, Salmonella sp., and E. coli* O157. These findings support the feasibility of producing biologically active CU1-related products through recombinant expression in *P. pastoris*, providing an alternative to extraction from its natural source. However, the native peptide and the recombinant fermentation supernatant differ in sample purity, concentration determination, and experimental conditions. Therefore, their antibacterial potencies cannot be directly compared on the basis of the reported MIC values alone.

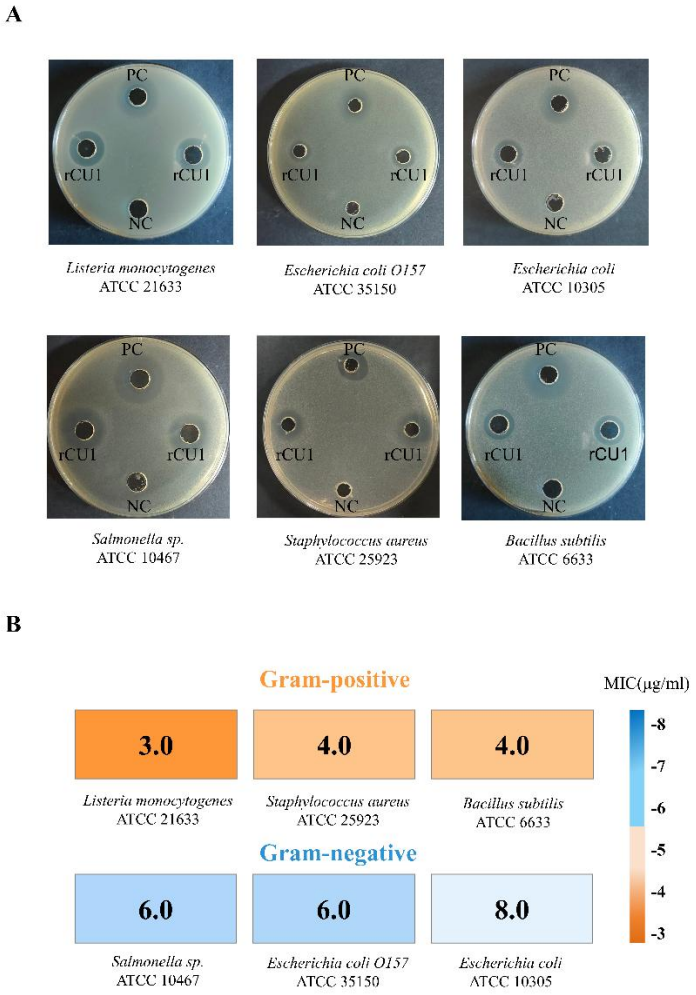


Figure 3. Antibacterial activity and minimum inhibitory concentrations (MICs) of CU1-containing fermentation supernatant (CU1-FS) against six bacterial strains. (A) Antibacterial activity of CU1-FS determined by the agar well diffusion assay. Bacterial species and strain designations are indicated below each image. PC, gentamicin (positive control); NC, culture supernatant from *Pichia pastoris* carrying the empty pPICZαA vector (negative control); rCU1, CU1-containing fermentation supernatant (CU1-FS). (B) MICs of CU1-FS against three Gram-positive and three Gram-negative bacterial strains. MIC values are expressed as the apparent concentrations of His-tagged recombinant products estimated by ELISA.

3.4 Stability of Recombinant Cliotide U1

The effect of temperature on the antibacterial activity of CU1-FS was first examined. Inhibition zone diameters remained relatively stable following treatment at 4 – 37℃ but gradually decreased as the temperature increased. After incubation at 50, 60, 80, and 100℃, the inhibition zone diameters were approximately 95%, 86%, 78%, and 70% of that observed for the 4℃ reference group, respectively (Fig. 4A). Although elevated temperatures reduced the antibacterial activity of CU1-FS, a measurable inhibition zone remained after treatment at 100℃ for 1 h, indicating that its antibacterial activity was partially preserved under high-temperature conditions. Taheri et al. reported that native CU1 maintained relatively stable antibacterial activity between 10 and 60℃, followed by a gradual decline at higher temperatures [20]. The present findings are consistent with the thermal tolerance reported for native CU1. However, because CU1-FS was tested as an unpurified fermentation supernatant, other components in the supernatant may have contributed to the observed stability. The thermal stability of purified recombinant CU1 therefore remains to be established.

The antibacterial activity of CU1-FS was also affected by pH treatment (Fig. 4B). A marked reduction in the inhibition zone diameter was observed following exposure to pH 2. In contrast, CU1-FS produced relatively large inhibition zones after treatment at pH 6 – 10, with the greatest diameters observed at pH 8 – 10. Although the inhibition zone diameter decreased at pH 12, antibacterial activity remained detectable. These observations indicate that CU1-FS maintained stronger antibacterial activity following exposure to near-neutral and alkaline conditions than under strongly acidic conditions. Environmental pH can alter the protonation states of amino acid side chains and influence peptide conformation, molecular interactions, and antibacterial activity. Such effects may contribute to the differences observed among the pH treatment groups. However,

because pH can also directly influence bacterial growth and inhibition zone formation, the present results do not establish whether the observed differences arise solely from changes in CU1 stability.

CU1-FS showed relatively little change in antibacterial activity following treatment with increasing NaCl concentrations (Fig. 4C). As the added NaCl concentration increased from 0 to 500 mmol/L, the inhibition zone diameter decreased only slightly, remaining at approximately 94% of the value measured without additional NaCl. This result indicates that CU1-FS maintained substantial antibacterial activity under the tested high-salt conditions. Ionic strength can influence the electrostatic attraction between cationic antimicrobial peptides and negatively charged bacterial surfaces, thereby affecting peptide–membrane interactions [38,39]. The relatively small reduction in inhibition zone diameter at elevated NaCl concentrations suggests that the antibacterial activity of CU1-FS is less sensitive to changes in ionic strength within the tested range. This property may be advantageous for further investigation of CU1-FS in environments where salt concentrations vary.

Protease treatment also affected the antibacterial activity of CU1-FS (Fig. 4D). Following exposure to pepsin, proteinase K, papain, and trypsin, the inhibition zone diameters remained approximately 77%–83% of that of the untreated CU1-FS group. Although a reduction was observed after enzymatic treatment, all four protease-treated samples retained detectable antibacterial activity, indicating partial tolerance to the tested proteolytic conditions. Proteolytic degradation is a major limitation in the development of antimicrobial peptides, particularly when they are intended for use in complex biological environments. Previous studies have therefore explored strategies to improve peptide resistance to proteolysis and preserve antibacterial activity [44,45]. The present results show that the antibacterial activity of CU1-FS was not completely lost following protease treatment. Nevertheless, the contribution of other fermentation supernatant

components and the extent of CU1 degradation require further investigation before the intrinsic proteolytic stability of the recombinant peptide can be established.

Overall, CU1-FS retained measurable antibacterial activity following exposure to elevated temperatures, different pH conditions, high NaCl concentrations, and proteolytic enzymes, although the extent of activity retention varied among treatments. Its performance under high-salt conditions was particularly notable, with only a small reduction in inhibition zone diameter at the highest NaCl concentration tested. These findings indicate that CU1-FS exhibits a degree of tolerance to different environmental conditions and provide a basis for further evaluating its antibacterial performance in more complex systems. Additional studies using purified recombinant CU1 will be necessary to distinguish the intrinsic stability of the peptide from potential protective effects of the fermentation supernatant.

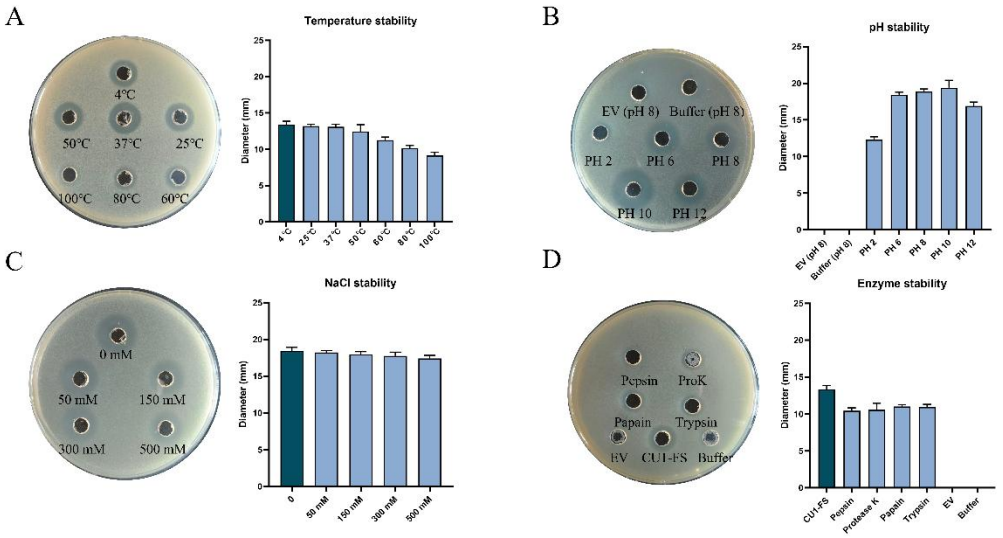


Figure 4. Effects of different treatments on the antibacterial activity of CU1-containing fermentation supernatant (CU1-FS). (A) Thermal stability. (B) Effect of pH. (C) Salt tolerance. (D) Protease stability. Antibacterial activity was evaluated against *Staphylococcus aureus* using the agar well diffusion assay. Representative inhibition zones and corresponding inhibition zone

diameters are shown. EV, fermentation supernatant from *Pichia pastoris* carrying the empty vector; CU1-FS, untreated CU1-containing fermentation supernatant.

3.5 Hemolytic Activity of CU1-Containing Fermentation Supernatant

The hemolytic activity of CU1-FS was evaluated using human erythrocytes. CU1-FS samples prepared at concentrations ranging from 0.78 to 12.6 μg/mL exhibited low hemolytic activity, with the percentage of hemolysis decreasing as the sample concentration declined (Fig. 5). The hemolysis rates were approximately 4.0%, 3.7%, 3.3%, 3.0%, and 2.1% for CU1-FS samples prepared at 12.6, 6.3, 3.15, 1.58, and 0.78 μg/mL, respectively. These values were substantially lower than that of the Triton X-100 positive control, while the CU1-free fermentation supernatant used as the negative control caused negligible hemolysis. Visual examination of the samples was consistent with the quantitative measurements. The supernatant of the positive control exhibited a pronounced red coloration, consistent with extensive erythrocyte lysis, whereas the CU1-FS-treated samples showed much lighter coloration, indicating limited disruption of erythrocyte membranes under the tested conditions.

Hemolytic activity is an important parameter for assessing the selectivity and preliminary biological safety of antimicrobial peptides toward host cells [46]. In the present study, CU1-FS exhibited low erythrocyte hemolysis under the experimental conditions, suggesting a relatively favorable preliminary hemolytic profile. Taheri et al. similarly reported limited hemolytic activity of native CU1 at relatively low concentrations [20]. Although the present findings are consistent with the low hemolytic activity previously reported for native CU1, differences in sample composition and experimental conditions should be considered when comparing the two studies. The observed antibacterial activity and low erythrocyte hemolysis of CU1-FS support further

investigation of its biological safety, particularly through studies using purified recombinant CU1 and additional host-cell models.

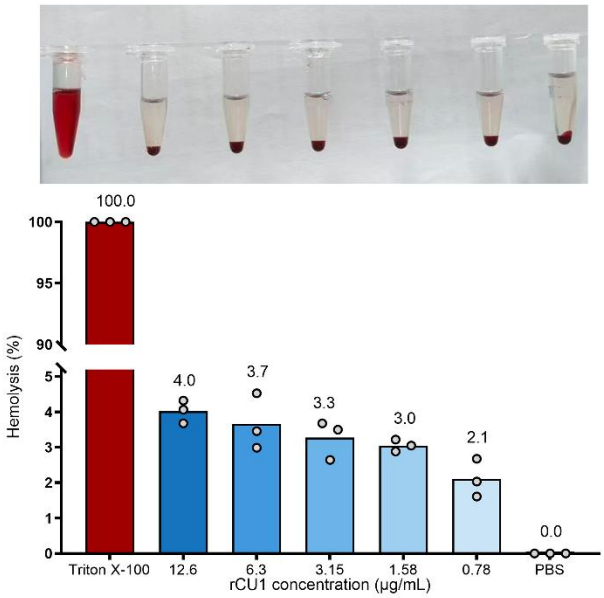


Figure 5. Hemolytic activity of CU1-FS against human erythrocytes.

Hemolysis induced by CU1-FS at different concentrations (0.78–12.6 μg/mL) was evaluated using human red blood cells. Triton X-100 was used as the positive control and PBS as the negative control. The upper panel shows representative images of erythrocyte suspensions after treatment, and the lower panel shows the corresponding hemolysis percentages.

3.6 Investigation of the Antibacterial Mechanism

3.6.1 Effects of CU1-FS on Bacterial Morphology and Membrane Permeability

Scanning electron microscopy (SEM) revealed that *Escherichia coli* cells treated with CU1-free control fermentation supernatant maintained a regular rod-shaped morphology with intact cell outlines, while *Staphylococcus aureus* cells exhibited a typical spherical shape with relatively smooth surfaces. Following treatment with CU1-FS at 1× MIC, both bacterial species showed

pronounced morphological alterations. *E. coli* cells displayed irregular contours, localized surface collapse, and cell aggregation, whereas *S. aureus* cells exhibited roughened surfaces, morphological deformation, and localized indentations (Fig. 6A). These structural changes indicate that CU1-FS treatment affects bacterial cell envelope integrity. Cationic amphipathic antimicrobial peptides commonly interact with negatively charged bacterial surfaces through electrostatic attraction, followed by hydrophobic interactions with the lipid bilayer that can lead to membrane disturbance [47,48]. As demonstrated by the preceding bioinformatic analysis, CU1 possesses a net positive charge, relatively high hydrophobicity, and a predominantly α-helical structure. These characteristics are consistent with those of membrane-active antimicrobial peptides and may contribute to the morphological changes observed after CU1-FS treatment.

Propidium iodide (PI) staining provided further evidence of changes in bacterial membrane permeability. Both *E. coli* and *S. aureus* cells treated with CU1-free control fermentation supernatant showed little detectable red fluorescence. In contrast, CU1-FS treatment markedly increased PI fluorescence intensity and the number of PI-positive cells in both bacterial species (Fig. 6B). PI is generally excluded by intact bacterial membranes but can enter cells with compromised membrane integrity and bind to intracellular nucleic acids. Increased PI uptake is therefore indicative of elevated membrane permeability [49]. While SEM revealed alterations in bacterial surface morphology, PI staining provided complementary evidence of impaired membrane barrier function. Together, these observations support membrane damage as an important component of the antibacterial action associated with CU1-FS treatment.

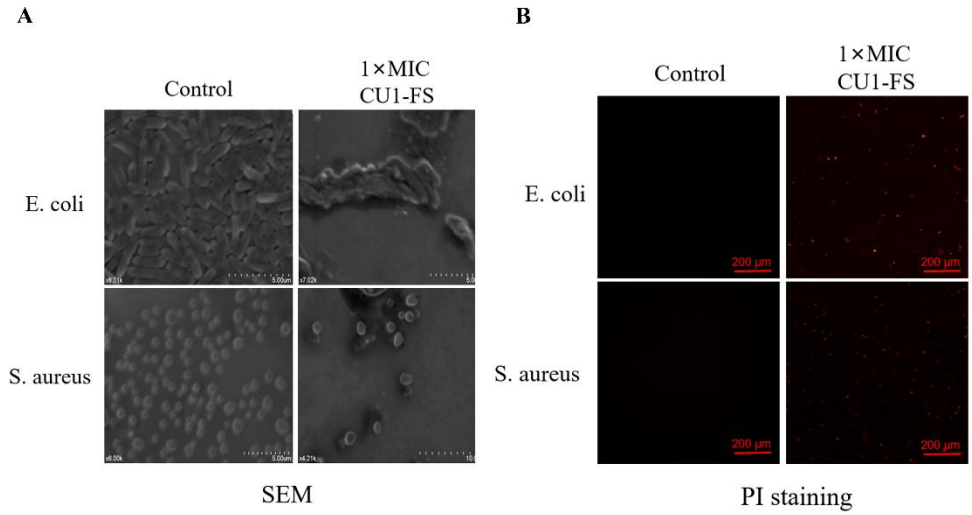


Figure 6. Effects of CU1-containing fermentation supernatant (CU1-FS) on bacterial morphology and membrane permeability. (A) Scanning electron microscopy (SEM) images showing morphological changes in *Escherichia coli* and *Staphylococcus aureus* following CU1-FS treatment. (B) Propidium iodide (PI) fluorescence staining showing changes in membrane permeability in *E. coli* and *S. aureus*. Control, bacterial cells treated with CU1-free fermentation supernatant; CU1-FS, bacterial cells treated with CU1-containing fermentation supernatant at 1× MIC.

3.6.2 CU1-FS-Induced Leakage of Intracellular Components and Its Interaction with Bacterial Genomic DNA

The leakage of intracellular components provided further evidence of impaired bacterial membrane barrier function following CU1-FS treatment. As the treatment duration increased, the OD260 and OD280 values of the Staphylococcus aureus supernatants generally increased. Specifically, OD260 increased from 10.178 at 1 h to 12.875 at 4 h, while OD280 increased from 7.369 at 1 h and remained relatively high at subsequent time points (Fig. 7A). A similar trend was observed in the concentration-dependent assay, where both OD260 and OD280 generally increased with increasing CU1-FS concentrations. In particular, OD260 increased from 1.835 at 0.79 μg/mL

to 11.492 at 12.6 μg/mL (Fig. 7B). These findings indicate increased release of nucleic acid- and protein-associated components into the extracellular environment following CU1-FS treatment, with overall time- and concentration-dependent trends. Compared with morphological alterations alone, the increased extracellular absorbance provides additional evidence that CU1-FS-induced membrane damage is accompanied by a loss of membrane barrier function.

In addition to membrane disruption, the DNA migration assay revealed a potential interaction between CU1-FS and bacterial genomic DNA. Genomic DNA extracted from Escherichia coli and S. aureus migrated normally through the agarose gel following incubation with CU1-free control fermentation supernatant. In contrast, increasing concentrations of CU1-FS altered DNA migration, with a portion of the DNA retained near the loading wells (Fig. 7C). Cationic antimicrobial peptides can interact with negatively charged DNA through electrostatic attraction and other noncovalent interactions, potentially forming peptide–DNA complexes that alter electrophoretic mobility. Previous studies have also demonstrated that certain antimicrobial peptides can interact with intracellular macromolecules, including DNA, in addition to disrupting bacterial membranes, providing evidence for multiple antibacterial targets [50,51]. The altered DNA migration observed in the present study therefore raises the possibility that CU1 may interact with bacterial DNA in addition to exerting membrane-associated effects.

It should be noted that the DNA interaction assay was performed using extracted bacterial genomic DNA under cell-free conditions. Thus, the present findings demonstrate that CU1-FS alters the electrophoretic migration of bacterial DNA but do not establish whether CU1 enters the cytoplasm of living bacterial cells or directly targets genomic DNA intracellularly. Further studies involving intracellular localization and direct DNA-binding assays are needed to determine whether

CU1 acts through a combination of membrane disruption and intracellular targeting. Such a mechanism could, in principle, reduce the likelihood of bacterial resistance arising through alterations in a single molecular target. However, this possibility remains to be tested through serial-passage experiments or experimental resistance-evolution assays.

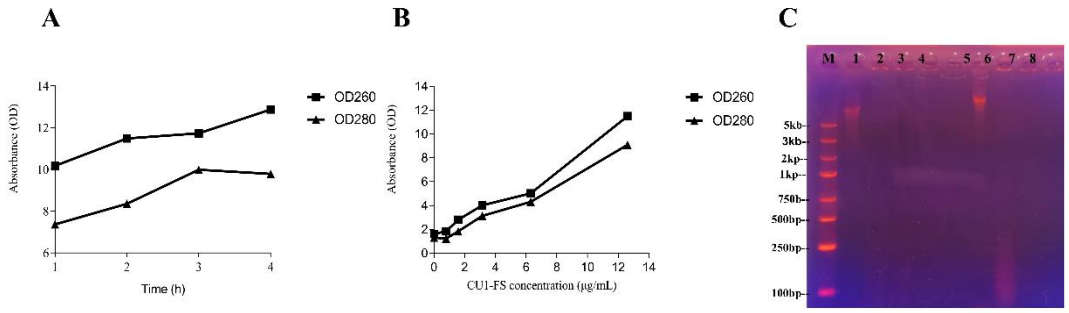


Figure 7. Effects of CU1-FS on intracellular component leakage and genomic DNA migration. (A) Time-dependent and (B) concentration-dependent changes in OD260 and OD280 in *Staphylococcus aureus* following CU1-FS treatment. (C) Agarose gel electrophoresis of *Escherichia coli* (lanes 1–4) and *S. aureus* (lanes 5–8) genomic DNA. M, DNA marker; lanes 1 and 5, negative controls; lanes 2–4 and 6–8, CU1-FS at 3.15, 6.3, and 12.6 μg/mL, respectively.

3.6.3 Molecular Docking Analysis of CU1 with Bacterial Proteins

To further investigate the potential interactions between CU1 and bacterial proteins, molecular docking was performed using the outer membrane porin F (OmpF) from *Escherichia coli* and sortase A from *Staphylococcus aureus* as receptor proteins. OmpF is an important channel-forming protein in the outer membrane of Gram-negative bacteria [52], whereas sortase A is involved in anchoring surface proteins to the cell wall of Gram-positive bacteria and contributes to bacterial cell surface organization [53]. These proteins were therefore selected as candidate models for exploring potential interactions between CU1 and bacterial envelope-associated proteins.

Molecular docking was performed using HDOCK [36]. The top-ranked CU1–OmpF complex exhibited a docking score of −324.55 and a confidence score of 0.9704. The predicted binding interface involved hydrogen bonds and other noncovalent interactions with residues including Arg42, Thr300, Tyr302, and Gln339 (Fig. 8A). For the CU1–sortase A complex, the top-ranked binding pose yielded a docking score of −229.43 and a confidence score of 0.8304, with predicted interactions involving Gly74, Tyr75, Glu85, and Tyr88 (Fig. 8B).

These results indicate that CU1 can adopt predicted binding conformations with both OmpF and sortase A, raising the possibility that its antibacterial activity may involve interactions with bacterial envelope-associated proteins in addition to membrane lipids. However, molecular docking provides computationally predicted binding modes rather than direct evidence of protein–peptide interactions, and docking scores should not be interpreted as experimentally determined binding free energies. OmpF and sortase A should therefore be regarded as candidate interaction partners rather than confirmed molecular targets of CU1. The predicted interactions provide a structural perspective complementary to the membrane-associated alterations observed in the preceding experiments and offer potential directions for further mechanistic investigation.

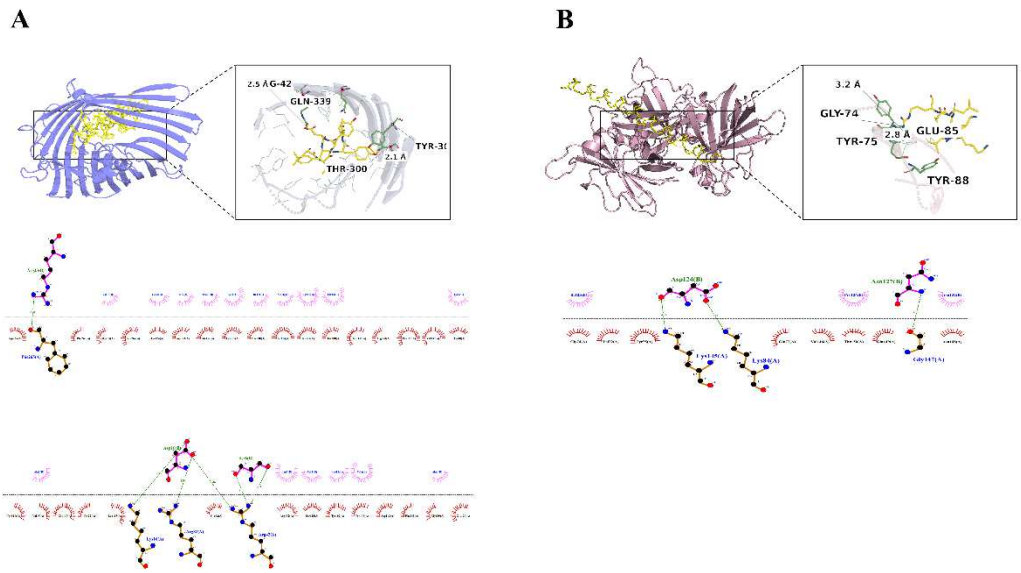


Figure 8. Molecular docking analysis of CU1 with bacterial envelope-associated proteins. (A) Predicted interactions between CU1 and *E. coli* OmpF. (B) Predicted interactions between CU1 and *S. aureus* sortase A. Three-dimensional binding poses, interacting residues, and corresponding two-dimensional interaction diagrams are shown.

3.6.4 Molecular Dynamics Analysis of CU1 – Lipid Membrane Interactions

To further characterize the dynamic interactions between CU1 and lipid membranes, a 100 ns molecular dynamics (MD) simulation was performed using a mixed POPE/POPG lipid bilayer model [37]. Representative snapshots showed that CU1 maintained contact with the lipid bilayer interface throughout the simulation (Fig. 9A, B). The radius of gyration (Rg) and root mean square deviation (RMSD) of CU1 remained within relatively stable ranges, without sustained large fluctuations (Fig. 9C, D), indicating that the peptide maintained a relatively stable overall conformation in the membrane environment. However, Rg and RMSD primarily describe the conformational behavior of CU1 itself and cannot directly establish whether structural damage

occurred in the lipid bilayer.

The number of hydrogen bonds between CU1 and the lipid membrane fluctuated throughout the simulation, reflecting the continuous formation and dissociation of hydrogen bonds at the peptide–membrane interface (Fig. 9E). Meanwhile, the solvent-accessible surface area (SASA) of CU1 remained relatively stable (Fig. 9F), suggesting that its overall solvent exposure did not undergo substantial changes. Considered together, the Rg, RMSD, hydrogen-bond, and SASA analyses indicate that CU1 maintained a relatively stable conformation while continuously interacting with membrane lipids.

The interaction of antimicrobial peptides with bacterial membranes commonly begins with peptide adsorption and accumulation at the membrane surface. Electrostatic attraction, hydrogen bonding, and hydrophobic interactions can subsequently stabilize peptide–membrane association and contribute to changes in lipid organization and membrane physical properties [43]. Previous studies have shown that the accumulation and sustained interactions of certain short antimicrobial peptides at membrane surfaces can induce localized membrane deformation and carpet-like membrane disruption [47]. Transient toroidal pores have also been reported in specific antimicrobial peptide systems [54]. However, the Rg, RMSD, hydrogen-bond, and SASA analyses performed in the present study primarily characterize the conformation of CU1 and its interactions with membrane lipids. These parameters alone do not provide direct evidence that CU1 induces membrane curvature or pore formation.

When considered alongside the morphological alterations observed by SEM, the increased membrane permeability detected by PI staining, and the leakage of intracellular components, these findings support the possibility that CU1 association with bacterial membranes and its continued

interactions with membrane lipids contribute to the disruption of membrane structure and barrier function. The simulations thus provide a molecular interpretation consistent with the membrane damage observed experimentally, although the precise structural changes induced in the lipid bilayer remain to be established.

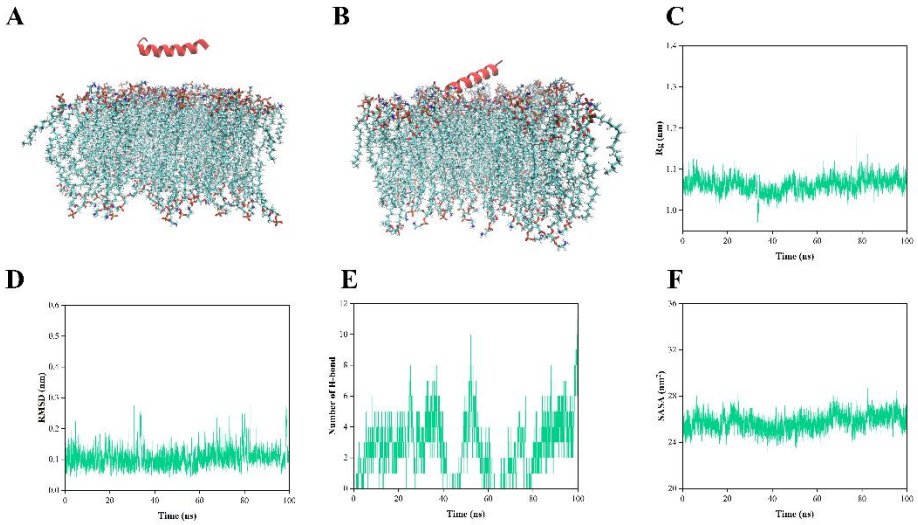


Figure 9. Molecular dynamics analysis of CU1 interactions with a POPE/POPG lipid bilayer. (A, B) Representative snapshots of the CU1–lipid bilayer system. (C) Radius of gyration (Rg). (D) Root mean square deviation (RMSD). (E) Number of hydrogen bonds between CU1 and membrane lipids. (F) Solvent-accessible surface area (SASA) of CU1 during the 100 ns simulation.

4. Conclusion

In this study, a recombinant expression system for Cliotide U1 (CU1) was established in Pichia pastoris, yielding a CU1-containing fermentation supernatant with antibacterial activity. CU1-FS exhibited inhibitory activity against all tested Gram-positive and Gram-negative bacterial strains,

with minimum inhibitory concentrations (MICs) ranging from 3 to 8 μg/mL. It also retained antibacterial activity following exposure to elevated temperatures, proteolytic enzymes, and high salt concentrations, while exhibiting low hemolytic activity against human erythrocytes under the tested conditions. Mechanistic investigations revealed that CU1-FS treatment induced morphological alterations in bacterial cells, increased membrane permeability, and promoted the leakage of intracellular components, supporting membrane damage as an important component of its antibacterial action. Changes in the electrophoretic migration of bacterial genomic DNA further indicated a potential interaction between CU1-FS and DNA. Molecular docking and molecular dynamics simulations provided additional structural and dynamic insights into the predicted interactions of CU1 with bacterial envelope-associated proteins and lipid membranes.

5. Limitations and Future Perspectives

Although this study established a recombinant expression system for CU1 and characterized the antibacterial properties of CU1-containing fermentation supernatant, several aspects require further investigation. As CU1-FS was not purified, the potential contribution of other fermentation supernatant components to its antibacterial activity and stability cannot be fully excluded. In addition, the DNA migration assay indicated a possible interaction with bacterial genomic DNA in vitro, but direct intracellular DNA targeting remains to be verified.

Future studies should focus on improving recombinant CU1 production, obtaining purified peptide for more precise functional characterization, and further clarifying its antibacterial mechanism. Evaluation of its efficacy and safety in relevant animal models will also be important for assessing its application potential. These investigations will provide a basis for the further development of CU1 as a peptide-based antibacterial candidate.

Acknowledgments

None.

Funding

This research did not receive any specific grant from funding agencies in the public, commercial, or not-for-profit sectors.

Conflict of Interest Statement

The authors declare that they have no known competing financial interests or personal relationships that could have appeared to influence the work reported in this paper.

Clinical trial number: not applicable.

References

[1] Larsson DGJ, Flach CF. Antibiotic resistance in the environment. Nat Rev Microbiol. 2022;20:257-269. doi: 10.1038/s41579-021-00649-x.

[2] Antimicrobial Resistance Collaborators. Global burden of bacterial antimicrobial resistance in 2019: a systematic analysis. Lancet. 2022;399(10325):629-655. doi: 10.1016/S0140-6736(21)02724-0.

[3]Holmes AH, Moore LS, Sundsfjord A, Steinbakk M, Regmi S, Karkey A, Guerin PJ, Piddock LJ. Understanding the mechanisms and drivers of antimicrobial resistance. Lancet. 2016;387(10014):176-187. doi: 10.1016/S0140-6736(15)00473-0.

[4] Klein EY, Van Boeckel TP, Martinez EM, Pant S, Gandra S, Levin SA, Goossens H, Laxminarayan R. Global increase and geographic convergence in antibiotic consumption between 2000 and 2015. Proc Natl Acad Sci U S A. 2018;115(15):E3463-E3470. doi: 10.1073/pnas.1717295115.

[5] GBD 2021 Antimicrobial Resistance Collaborators. Global burden of bacterial antimicrobial resistance 1990–2021: a systematic analysis with forecasts to 2050. The Lancet. 2024;404(10459):1199–1226.

[6] Cabello FC. Heavy use of prophylactic antibiotics in aquaculture: a growing problem for human and animal health and for the environment. Environ Microbiol. 2006;8:1137-1144. doi: 10.1111/j.1462-2920.2006.01054.x.

[7] Lulijwa R, Rupia EJ, Alfaro AC. Antibiotic use in aquaculture, policies and regulation, health and environmental risks: a review of the top 15 major producers. Rev Aquac. 2020;12:640-663. doi: 10.1111/raq.12344.

[8] Marshall BM, Levy SB. Food animals and antimicrobials: impacts on human health. Clinical Microbiology Reviews. 2011;24(4):718–733. https://doi.org/10.1128/cmr.00002-11

[9] Hancock RE, Sahl HG. Antimicrobial and host-defense peptides as new anti-infective therapeutic strategies. Nat Biotechnol. 2006;24(12):1551-1557. doi: 10.1038/nbt1267.

[10] Huan Y, Kong Q, Mou H, Yi H. Antimicrobial Peptides: Classification, Design, Application and Research Progress in Multiple Fields. Front Microbiol. 2020;11:582779. doi: 10.3389/fmicb.2020.582779.

[11] Mookherjee N, Anderson MA, Haagsman HP, Davidson DJ, Bals R, Hancock REW. Antimicrobial host defence peptides: functions and clinical potential. Nat Rev Drug Discov. 2020;19(5):311-332. doi: 10.1038/s41573-019-0058-8.

[12] Brian P. Lazzaro et al. ,Antimicrobial peptides: Application informed by evolution.Science368,eaau5480(2020).DOI:10.1126/science.aau5480

[13]Lei J, Sun L, Huang S, et al. The antimicrobial peptides and their potential clinical applications. Am J Transl Res. 2019;11(7):3919-3931.

[14]Brogden, K. Antimicrobial peptides: pore formers or metabolic inhibitors in bacteria?. Nat Rev Microbiol 3, 238–250 (2005). https://doi.org/10.1038/nrmicro1098

[15] Magana M, Pushpanathan M, Santos AL, et al. The value of antimicrobial peptides in the age of resistance. Lancet Infect Dis. 2020;20(9):e216-e230. doi: 10.1016/S1473-3099(20)30327-3.

[16] Rosano GL, Morales ES, Ceccarelli EA. New tools for recombinant protein production in Escherichia coli: A 5-year update. Protein Sci. 2019;28(8):1412-1422. doi: 10.1002/pro.3668.

[17] Li Y. Recombinant production of antimicrobial peptides in Escherichia coli: A review. Protein Expr Purif. 2011;80(2):260-267. doi: 10.1016/j.pep.2011.08.001.

[18] Baghban R, Farajnia S, Rajabibazl M, Ghasemi Y, Mafi A, Hoseinpoor R, Rahbarnia L, Aria M. Yeast Expression Systems: Overview and Recent Advances. Mol Biotechnol. 2019 May;61(5):365-384. doi: 10.1007/s12033-019-00164-8. PMID: 30805909.

[19] Karbalaei M, Rezaee SA, Farsiani H. Pichia pastoris: A highly successful expression system for optimal synthesis of heterologous proteins. J Cell Physiol. 2020;235(9):5867-5881. doi: 10.1002/jcp.29583.

[20] Taheri MN, Seyedjavadi SS, Goudarzi M, Ebrahimipour G, Hashemi A. Cliotide U1, a Novel Antimicrobial Peptide Isolated From Urtica Dioica Leaves. Bioinform Biol Insights. 2025;19:11779322251315291. doi: 10.1177/11779322251315291.

[21] Gasteiger E, Hoogland C, Gattiker A, Duvaud S, Wilkins MR, Appel RD, Bairoch A. Protein Identification and Analysis Tools on the ExPASy Server. In: Walker JM, ed. The Proteomics Protocols Handbook. Humana Press; 2005:571-607. doi: 10.1385/1-59259-890-0:571

[22] Geourjon C, Deléage G. SOPMA: significant improvements in protein secondary structure prediction by consensus prediction from multiple alignments. Comput Appl Biosci. 1995;11(6):681-684. doi: 10.1093/bioinformatics/11.6.681.

[23] Lamiable A, Thévenet P, Rey J, Vavrusa M, Derreumaux P, Tufféry P. PEP-FOLD3: faster de novo structure prediction for linear peptides in solution and in complex. Nucleic Acids Res. 2016;44(W1):W449-W454. doi: 10.1093/nar/gkw329.

[24] Kyte J, Doolittle RF. A simple method for displaying the hydropathic character of a protein. Journal of Molecular Biology. 1982;157(1):105–132. doi:10.1016/0022-2836(82)90515-0.

[25] Blom N, Gammeltoft S, Brunak S. Sequence and structure-based prediction of eukaryotic protein phosphorylation sites. Journal of Molecular Biology. 1999;294(5):1351–1362.

[26] Teufel F, Almagro Armenteros JJ, Johansen AR, et al. SignalP 6.0 predicts all five types of signal peptides using protein language models. Nature Biotechnology. 2022;40:1023–1025. doi:10.1038/s41587-021-01156-3.

[27] Hallgren J, Tsirigos KD, Pedersen MD, et al. DeepTMHMM predicts alpha and beta transmembrane proteins using deep neural networks. bioRxiv. 2022. doi:10.1101/2022.04.08.487609.

[28] Gupta S, Kapoor P, Chaudhary K, et al. In silico approach for predicting toxicity of peptides and proteins. PLoS ONE. 2013;8(9):e73957. doi:10.1371/journal.pone.0073957.

[29] Dimitrov I, Bangov I, Flower DR, Doytchinova I. AllerTOP v.2—a server for in silico prediction of allergens. Journal of Molecular Modeling. 2014;20:2278. doi:10.1007/s00894-014-2278-5.

[30] Zhang S, Lin R, Cui L, Jiang T, Shi J, Lu C, Li P, Zhou M. Alter codon bias of the P. pastoris genome to overcome a bottleneck in codon optimization strategy development and improve protein expression. Microbiol Res. 2024;282:127629. doi: 10.1016/j.micres.2024.127629.

[31] Schägger H. Tricine-SDS-PAGE. Nat Protoc. 2006;1(1):16-22. doi: 10.1038/nprot.2006.4.

Engvall E, Perlmann P. Enzyme-linked immunosorbent assay (ELISA). Quantitative assay of immunoglobulin G. Immunochemistry. 1971;8(9):871–874. doi:10.1016/0019-2791(71)90454-X.

[33] Lian K, Wang Y, Jiao Y, et al. Identification and expression of a novel antimicrobial peptide Gloverin and its antibacterial effect against Staphylococcus aureus. BMC Microbiology. 2025;25(1):554.

[34] Hu M, Cha S, Li Y, et al. A food-grade antimicrobial peptide from Lactococcus lactis: a potent and stable bio-preservative against Gram-negative pathogens in orange juice. Food Control. 2026;183(1):111922.

[35] Abramson J, Adler J, Dunger J, et al. Accurate structure prediction of biomolecular interactions with AlphaFold 3. Nature. 2024;630:493 – 500. doi:10.1038/s41586-024-07487-w.

[36] Yan Y, Zhang D, Zhou P, Li B, Huang SY. HDOCK: a web server for protein – protein and protein – DNA/RNA docking based on a hybrid strategy. Nucleic Acids Research. 2017;45(W1):W365 – W373. doi:10.1093/nar/gkx407.

[37] Abraham MJ, Murtola T, Schulz R, et al. GROMACS: High performance molecular simulations through multi-level parallelism from laptops to supercomputers. SoftwareX. 2015;1 – 2:19 – 25. doi:10.1016/j.softx.2015.06.001.

[38] Oliveira Júnior NG, Souza CM, Buccini DF, Cardoso MH, Franco OL. Antimicrobial peptides: structure, functions and translational applications. Nat Rev Microbiol. 2025;23(11):687 – 700. doi:10.1038/s41579-025-01200-y.

[39] Gu R, Gao B, Wang Z, et al. Plant-Derived Antimicrobial Peptides: Mechanism of Action, Safety and Integrated Applications. J Agric Food Chem. 2025;73(43):27161 – 27176. doi:10.1021/acs.jafc.5c06949.

[40] Leite ML, Oliveira KBS, Lima LF, Melo NTM, Brango-Vanegas J, Paes HC, Franco OL. Komagataella phaffii as a microbial cell factory for antimicrobial peptide production. J Biotechnol. 2025;408:275 – 287. doi:10.1016/j.jbiotec.2025.09.015.

[41] Li X, Hao Y, Teng D, Mao R, Yang N, Wang J. Review on microbial recombination expression of antimicrobial peptides. Chem Eng J. 2025. doi:10.1016/j.cej.2025.170733.

[42] Li M, Zhou R, Wang Y, Lu Y, Chu X, Dong C. Heterologous expression of frog antimicrobial peptide Odorranain-C1 in Pichia pastoris: Biological characteristics and its application in food preservation. J Biotechnol. 2024;390:50–61. doi:10.1016/j.jbiotec.2024.05.009.

[43] Yang R, Ma X, Peng F, Wen J, Allahou LW, Williams GR, Knowles JC, Poma A. Advances in antimicrobial peptides: From mechanistic insights to chemical modifications. Biotechnology Advances. 2025;81:108570. doi:10.1016/j.biotechadv.2025.108570.

[44] Wang J, Song J, Yang Z, He S, Yang Y, Feng X, Dou X, Shan A. Antimicrobial Peptides with High Proteolytic Resistance for Combating Gram-Negative Bacteria. J Med Chem. 2019;62(5):2286–2304. doi:10.1021/acs.jmedchem.8b01348.

[45] Ouyang X, Yuan L, Yang T, Xu Q, Li B, Zhang J, et al. Fluorinated Modification as a Simple Strategy That Effectively Enhances the Stability and Activity of Antimicrobial Peptides. J Med Chem. 2025;68(19):20081–20102. doi:10.1021/acs.jmedchem.5c00922.

[46] Kim SH, Min YH, Park MC. Antimicrobial Peptides: Current Status, Mechanisms of Action, and Strategies to Overcome Therapeutic Limitations. Microorganisms. 2025;13(11):2574. doi:10.3390/microorganisms13112574.

[47] Park P, Matsubara DK, Barzotto DR, Lima FS, Chaimovich H, Marrink SJ, Cuccovia IM. Vesicle protrusion induced by antimicrobial peptides suggests common carpet mechanism for short antimicrobial peptides. Sci Rep. 2024;14(1):9701. doi:10.1038/s41598-024-60601-w.

[48] Kumari S, Booth V. Antimicrobial Peptide Mechanisms Studied by Whole-Cell Deuterium NMR. Int J Mol Sci. 2022;23(5):2740. doi:10.3390/ijms23052740.

[49] Stiefel P, Schmidt-Emrich S, Maniura-Weber K, Ren Q. Critical aspects of using bacterial cell viability assays with the fluorophores SYTO9 and propidium iodide. BMC Microbiology.

2015;15:36. doi:10.1186/s12866-015-0376-x.

[50] Beyer LI, Thoma J, Acha Alarcon L, Unksov IN, Karlsson R, Inda-Díaz JS, Tietze AA. Marine-Inspired Antimicrobial Peptides Disrupt Gene Expression at the DNA Level. ACS Infect Dis. 2026;12(1):447–459. doi:10.1021/acsinfecdis.5c01000.

[51] Ma M, Song J, Xiao Y, Liu J, Hu Z, Zeng B. Multi-target action of novel antimicrobial peptide N1-5W6L-LKKFA against Escherichia coli O157:H7: Membrane disruption, ROS accumulation, DNA binding, cellular interference, and its application in milk. Innov Food Sci Emerg Technol. 2026;109:104448. doi:10.1016/j.ifset.2026.104448.

[52] Nikaido H. Molecular basis of bacterial outer membrane permeability revisited. Microbiology and Molecular Biology Reviews. 2003;67(4):593–656. doi:10.1128/MMBR.67.4.593-656.2003.

[53] Mazmanian SK, Liu G, Ton-That H, Schneewind O. Staphylococcus aureus sortase, an enzyme that anchors surface proteins to the cell wall. Science. 1999;285(5428):760–763. doi:10.1126/science.285.5428.760.

[54]Zan B, Chen CH, Mateen AI, Kolenovic B, Wiedman GR, Ulmschneider MB, Ulmschneider JP. PGLa and Magainin 2 Can Porate Membranes via Transient Hourglass-Shaped Toroidal Pores. J Am Chem Soc. 2026;148(2):2191–2205. doi:10.1021/jacs.5c11101.

Supplementary Files

This is a list of supplementary files associated with this preprint. Click to download.

- SupplementaryFile1.docx